

# INTERACTIVE VISUALIZATION OF RETINAL ASTROCYTE IMAGES

P. Suwannatat\*, G. Luna\*<sup>†</sup>, B. Ruttenberg\*, R. Raviv<sup>†</sup>, G. Lewis\*<sup>†</sup>, S.K. Fisher\*<sup>†</sup>, and T. Höllner\*<sup>†</sup>

\*Department of Computer Science, <sup>†</sup>Department of Electrical and Computer Engineering,  
<sup>\*†</sup>Neuroscience Research Institute, University of California, Santa Barbara

## ABSTRACT

Analyzing high-resolution images of astrocytes is important in understanding the diseases, such as glaucoma and retinal detachment, to which astrocytes are known to become reactive. This is challenging because the cells are small, homogeneous, and closely packed. We propose an interactive visualization system designed for such images. Our system employs a probabilistic segmentation algorithm to help distinguish between cells. Design decisions on visualization and interactions were made based on the needs of the scientists, resulting in a visualization that shows the details of individual cells in the context of a large image mosaic. Our interactive system brings patterns of information to the surface, conveys uncertainty, and serves as a tool for astrocyte research.

*Index Terms*— Astrocytes, Retina, Visualization

## 1. INTRODUCTION

Astrocytes are an important type of glial cell present in retinas. In addition to being involved in retinal vascular growth [1], astrocytes play an important role in diseases and injuries: glaucomatous neurodegeneration [2] and retinal detachment [3]. Studying astrocytes may elucidate their role in these conditions, yet there is a lack of tools for visualizing astrocytes effectively. Although biomedical imaging techniques have improved greatly since Stone and Dreher (1987) studied the distribution of astrocytes [4], work analyzing astrocyte images such as [1] still visualizes astrocyte network as a whole without distinguishing between individual cells. As data is gathered at higher resolution, the need for an interactive visualization tool designed specifically for astrocytes is paramount. Such a tool must integrate relevant image processing techniques, visualize each piece of data in context of the whole set, and be able to communicate uncertainty in the data.

We present an interactive visualization system designed for astrocyte images. Fig. 1 describes the pipeline where a mouse retina is stained, imaged, segmented, and visualized. Fig. 1(a) shows the astrocytes in green and blood vessels in blue. The astrocytes in 1(b) are segmented using a probabilistic method, resulting in images of individual cells as shown

in 1(c). The segmented cells are put together in 1(d), an inset of Fig. 2, showing cells in different colors. We implemented different visualization and interaction techniques, described in Section 4, to aid the exploration of the data. Section 5 describes how our software can show data in context, bring various patterns to the surface, and can potentially help in an investigation of detached retinas.

## 2. IMAGE COLLECTION

We are focusing on visualizing astrocytes of the whole retina. In order to compile a dataset, a mouse's retina tissue was fixed and stained with anti-GFAP for astrocytes, anti-collagen IV for blood vessels. As the astrocyte's cytoskeleton contains the protein GFAP, all astrocytes in the retina were visible.

The retina was then wholemounted and the astrocyte layer imaged at 40X magnification on a laser scanning confocal microscope Olympus FluoView 1000. Sections of  $\sim 316 \times \sim 316 \mu\text{m}$  were imaged at 20% overlap in X-Y and in 20, 0.5  $\mu\text{m}$  Z-steps, resulting in several hundred 3D images. The images were then stitched together into four large images using [5]. The resulting images were then Z-projected into a 2D image, as the astrocytes are very planar cells. Each image is a quadrant of the retina, approximately  $\sim 8500 \times \sim 4000$  pixels. This image resembles Fig. 2 but all astrocytes are in green as in Fig. 1(a).

## 3. CELL SEGMENTATION

The centers of the astrocytes in the images were manually marked, and each astrocyte was segmented out of the images using a probabilistic segmentation method [6]. This is a step in the pipeline from (b) to (c) in Fig. 1.

Probabilistic segmentation utilizes random walks with restart to demarcate each cell in the image. A  $1000 \times 1000$  pixel region  $R_i$  was extracted around each marked cell in the image, and a random walk was performed for each cell. The random walk method starts at the center of each cell (pixel (500, 500) of  $R_i$ ) and randomly moves to a neighboring pixel  $p_j$ , weighted on the intensity of the fluorescence at each pixel. After a move, the weights are recalculated using the new neighboring pixels, and another random move is performed. In addition, at each  $p_j$ , there is a small probability

This work is funded in part by NSF grant #0808762.

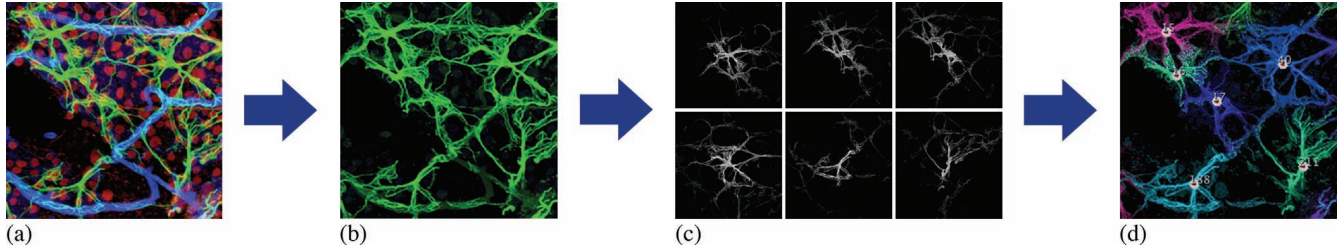


Fig. 1. Data pipeline from segmentation to visualization.

of moving directly to the pixel at the center of  $R_i$ . This process is repeated for thousands of iterations, and the number of times each cell is visited is recorded. The recorded visits are normalized with respect to the pixel at the center of  $R_i$ . The final result is that every pixel  $p_j \in R_i$  is assigned a probability of being part of the cell that  $R_i$  was extracted around. In Fig. 1(b), the six cells were extracted into probability maps represented by grayscale images in (c). We executed the random walk processes for the cells parallelly on a cluster; on average, this takes two minutes per cell.

The regions around each cell may overlap, hence there may be multiple values assigned to a pixel  $p_j$  via several random walks starting from different cells. We then normalize these values to sum to one in order to create a probability distribution for each  $p_j$ . That is, we assigned each pixel in the entire image a probability of assignment to each cell in the entire retina. For example, let us assume the random walk from cell  $A$  assigned a probability of 0.25 to pixel  $p_j$ , and the random walk from cell  $B$  also assigned a probability of 0.10 to  $p_j$ . Then normalizing these values, we determine that  $p_j$  is part of cell  $A$  with a  $\sim 0.71$  probability, part of cell  $B$  with a  $\sim 0.29$  probability, and zero for all other cells. Very small values below a threshold  $t$  are set to zero to avoid the scenario where a pixel with a very small probability of being assigned to only one cell is normalized, resulting in a probability of one. The next section describes how the images in Fig. 1(c) are combined to produce 1(d), an inset of Fig. 2.

#### 4. INTERACTIVE VISUALIZATION

The visualization’s primary goal is an in-context presentation of data so underlying patterns can emerge. This includes patterns of cell shapes, wrapping patterns around blood vessels, and patterns of cell density. These patterns are brought to the surface in Fig. 2, enhanced by interaction techniques that allow for a detailed view such as in Fig. 4(a). Since the segmentation algorithm we use is probabilistic, it is important to convey the amount of uncertainty as in Fig. 3. In Section 4.1, we describe how we put segmentation results together to create Fig. 2, which is not just an image but an interactive panel as explained in Section 4.2. In Section 4.3, we define uncertainty in our data and visualize it.

#### 4.1. Visualization techniques

To show the cell shapes and density patterns in context, we put the segmentation results from Section 3 together in a single big image. The image in Fig. 2 is rendered in accordance with design decisions made in iterative prototyping between computer scientists and biologists. Referring to the data pipeline in Fig. 1, we describe how we construct 1(d) from 1(c).

The combined image (Fig. 1(d)) has the same dimension as the original image (Fig. 1(b)). Each pixel, instead of containing a single color denotation, contains a linked list to pairs of  $(id, p)$  where  $p$  is the probability of  $cell_{id}$  occupying that pixel.

In rendering the final image as in Fig. 1(d) (inset of 2), the colors (hues) of different cells are initially randomly assigned. Since each pixel can be assigned to different cells, the color of the pixel is chosen to be the hue value of the cell whose probability is the greatest (called *the winning cell*). The brightness of the color is then proportional to such score. These design decisions conform with the principle that hue is suitable for distinguishing category while brightness is suitable for representing continuous quantity.

To avoid neighboring cells having similar colors, we experimented with different methods of assigning hues to the cells. A graph of cells are made based on their overlaps. A hue value is picked randomly for each cell, and then checked if it distinguishes the cell from its connected neighbors. We iterate until scores stop improving. Note that Vertex Coloring is NP-Complete and the overlap graph is non-planar, hence the chromatic number is not known easily. The users can also change the colors manually.

#### 4.2. Interactions

A variety of simple interaction techniques help the user explore the data both in detail and in context. Layers of information can be turned on by control panel switches, keyboard shortcuts, or mouse gestures.

In the default mode, the user sees a simple view as in Fig. 2, but the user can also bring up the cell center locations as shown in Fig. 1(d). As the user hovers the mouse over the image, the active cell becomes highlighted. The pixel boundary of the segmented cell is highlighted and its extent outlined by

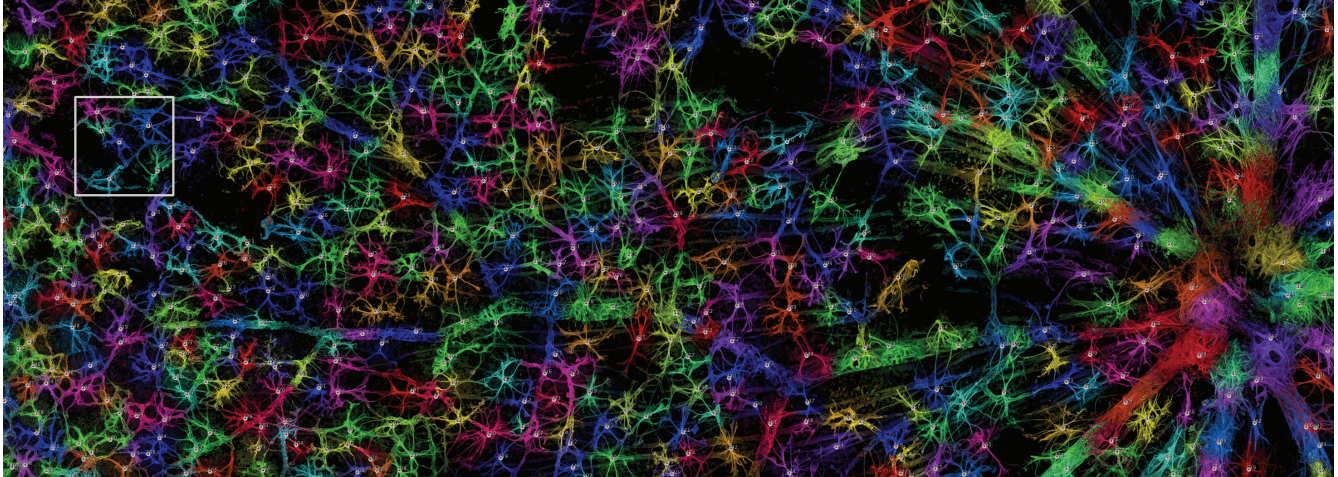


**Fig. 2.** Segmented astrocytes are assigned individual colors (hues). The centers of 535 cells are highlighted.

drawing its convex hull. The cell area is calculated by counting the number of pixels belonging to the cell, then converted to square microns and shown in a box. In Fig. 4(a), the user is viewing the detail of cell 40 (also the cell in the upper-right corner of the inset in Fig. 2), as well as performing a distance measurement of the diameter.

A selection of multiple cells can be toggled by double clicking at the cell centers. The user can also compare how the cell boundary is related to a Voronoi diagram of the cell centers in Fig. 4(b). When the feature is turned on, as the mouse hovers, the centers of the cells to which this pixel belong are highlighted with lines linked to the cells and the probability from the segmentation algorithm annotated.

### 4.3. Uncertainty Visualization

The uncertainty of our data comes from the fact that we assign colors to pixels based on the result of a probabilistic segmentation method. Cells overlap more heavily in some areas than others; therefore, the confidence in our decision to assign colors to a region varies across the image. For the sake of validity of any scientific conclusions drawn from the image, it is important that the amount of uncertainty be communicated to the user. We utilize the concept of entropy to quantify uncertainty. For each pixel, the entropy is defined as the random walk score of the winning cell divided by the sum of the random walk scores of all cells with respect to this pixel. The entropy is high when it is clear which cell occupies the pixel. To visualize, the image is divided into  $k \times k$ -pixel grids ( $k$  adjustable by the user), each cell displaying a glyph (a solid disc) whose size is inversely proportional to the average entropy. Fig. 3 overlays the image with glyphs of varying sizes. Wherever a glyph is big, the uncertainty is high – there are contentions between nearby cells so the cell color assignments should not be trusted completely.

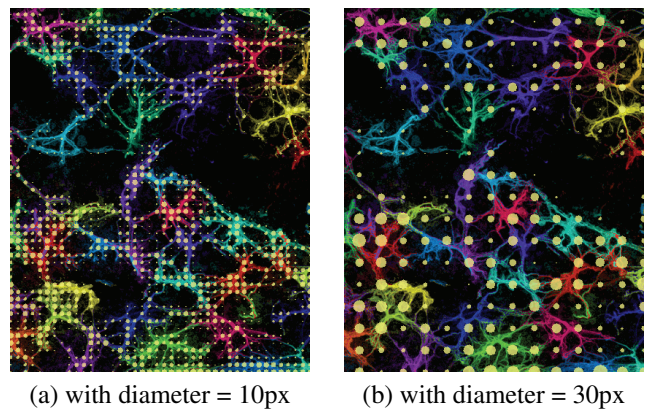


**Fig. 3.** Large glyphs appear where segmentation is uncertain.

## 5. RESULTS AND FEEDBACK

The authors who work in the field of biological research collaborate closely with the authors in computer science. The visualization system has been informally evaluated throughout by iterative prototyping. In this section, we describe how the system has been used and how it may aid in the analysis of new data.

Compared with traditional visualization methods for astrocytes, we find that our image of the individually segmented cells communicates effectively in the following overall areas: a) information about the individual cells such as shape and size; and b) the relationship between cells such as connectivity patterns and density variations.

Traditionally, individual images from the microscope are viewed independently, losing the context. An alternative method is to view a mosaic of those pictures, revealing the network of astrocytes but losing the details of individual cells.

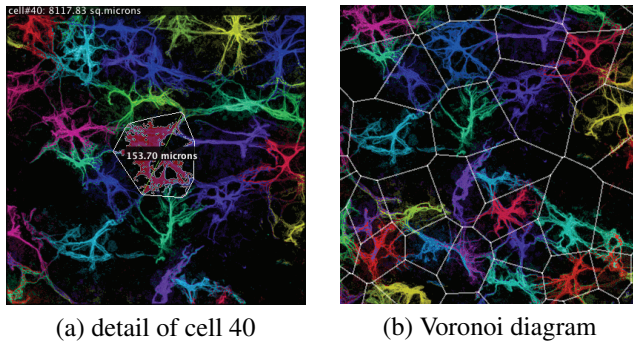


**Fig. 4.** Other visualization features

This problem is particularly severe for astrocytes because the cells are small, homogeneous (most cells look similar), and closely packed.

With our visualization system where cells are individually colored, we are able to see the shapes of individual cells while maintaining the global information such as the connectivity patterns and cell density. Generally, we are able to take advantage of the human ability to detect patterns both on global and local scale. For example, astrocytes along a blood vessel appear to have a certain shape, indicating a certain wrapping pattern running East-West about  $\frac{1}{3}$  from the bottom (See Fig. 2). On a global scale, the astrocytes tend to cluster around branches of the blood vessels, introducing areas of low density such as the dark area near the top right corner of Fig. 2.

By such visualization of multiple healthy retinas, the human observer can learn standard patterns of astrocyte shape, size, connectivity, density, and how the processes wrap around the blood vessels. This can potentially allow for a detection of changes in patterns across time of development and/or across animals with different conditions (e.g. aging, injury, disease, etc). A key question is whether an injury to the retina would cause homogeneous responses from all astrocytes. To answer this, not only do we need the images of normal vs. injured retinas, but also a tool that brings the patterns of changes to the surface of human perception.

Finally, there is a need in the research community for a communication medium among scientists. Our visualization system, by nature of its image occupying a large area of the retina, serves as a reference frame when hypotheses are formed or findings are described. While some interactive tools such as distance and area measurements can help communicate quantitative observations, other tools that show global patterns such as a Voronoi diagram (Fig. 4(b)) and the entropy glyphs can also help with qualitative discoveries.

## 6. CONCLUSION

Having collected an extensive set of images of mouse retinas, we developed an interactive visualization system that al-

lows the researcher to examine the data more effectively. By adapting state-of-the-art image processing techniques and integrating them with case-specific visualization and interaction techniques in a novel way, we are able to show the details of individual astrocytes – their shapes, areas, convex hull boundaries, and the uncertainty in segmentation – in the context of a larger area. We allow the patterns in the data to emerge so the scientists can draw observations regarding shape, size, connectivity, and density around blood vessels, as well as to detect such changes across time and conditions.

Our future work will incorporate a more streamlined data pipeline from raw data to visualization, an interface that more readily supports a larger data set of a whole retina at full resolution, interactive glyphs that show a summarization of data at a global scale while allowing the user to riffle through individual pieces of data, and a better interface for searching, sorting, and selecting cells. Cell center identification can be automated for our new genetically modified mice, whose nuclei react to a different stain. We will also improve the coloring of cells to minimize color collisions.

## 7. REFERENCES

- [1] Y. Kubota and T. Suda, “Feedback mechanism between blood vessels and astrocytes in retinal vascular development,” *Trends in Cardiovascular Medicine*, vol. 19, no. 2, pp. 38 – 43, 2009.
- [2] G. Prasanna, R. Krishnamoorthy, and T. Yorio, “Endothelin, astrocytes and glaucoma,” *Experimental Eye Research*, vol. In Press, Corrected Proof, 2010.
- [3] T. Nakazawa, M. Takeda, G. P. Lewis, K. S. Cho, J. Jiao, U. Wilhelmsson, S. K. Fisher, M. Pekny, D. F. Chen, and J. W. Miller, “Attenuated glial reactions and photoreceptor degeneration after retinal detachment in mice deficient in glial fibrillary acidic protein and vimentin,” *Investigative Ophthalmology and Visual Science*, vol. 48, no. 6, pp. 2760–2768, June 2007.
- [4] J. Stone and Z. Dreher, “Relationship between astrocytes, ganglion cells and vasculature of the retina,” *The Journal of Comparative Neurology*, vol. 255, no. 1, pp. 35 – 49, 1987.
- [5] M. Emmenlauer, O. Ronneberger, A. Ponti, P. Schwarb, A. Griffa, A. Filippi, R. Nitschke, W. Driever, and H. Burkhardt, “XuvTools: free, fast and reliable stitching of large 3 D datasets,” *Journal of Microscopy(Oxford)*, vol. 233, no. 1, pp. 42–60, 2009.
- [6] V. Ljosa and A.K. Singh, “Probabilistic segmentation and analysis of horizontal cells,” *Proceedings of the 6th IEEE International Conference on Data Mining, 2006*, pp. 980–985, Dec. 2006.